

# A comparative study using FEA on Tibia bone of different aged siblings

Suresh Guluwadi<sup>1</sup>Natnael mesfin<sup>2</sup>Jayakiran Reddy E<sup>3</sup>

1. Department of Mechanical Engineering, Adama Science and Technology University, Adama Ethiopia,

2. Department of Mechanical Engineering, Adama Science and Technology University, Adama Ethiopia,

3. Department of Mechanical Engineering, Sreenidhi Institute of Science and Technology, Hyderabad, Telangana, India

**Abstract**-A study of the human body tibia bone of three siblings (male, female, and child boy) is provided in this research. The male, female, and child boy are 23, 21, and 12 years old, respectively. Through 3D modelling, the authors were able to learn more about the tibia bone's behavior. CT scan data and DICOM pictures were used to generate a 3D model of the tibia bone. Finite element analysis is used to examine deformation, von-Mises stress, and factor of safety when a static load is applied. The findings of this study may benefit orthopedic surgeons in determining the load-bearing capability of the tibia bone in a single-family male, female, and child boy.

**Keywords:**Tibia bone, DICOM, CT Scan, Siblings.

## 1. INTRODUCTION

Different bones and muscles make up the human body. The tibia bone is one of the key bones in the lower leg that carries the majority of the bodyweight when a person stands or walks. In vertebrates, the tibia (shinbone) is the larger, stronger, and more anterior (frontal) of the two bones (Fibula and Tibia) that connect the knee and ankle bones. The tibia and fibula bones are shown in Figure 1. The tibia lies adjacent to the fibula on the medial side of the leg, closer to the median plane or midline. The tibia and fibula are connected by the interosseous membrane of the leg, resulting in a syndesmosis, a form of fibrous joint with limited mobility. The tibia is named after the tibia of the flute.



Figure 1. Position of the tibia bone in a human body (shown in red) [1].

The tibia is the human body's most powerful and second largest bone. The tibia is a long bone with two epiphyses and a diaphysis on each end. The diaphysis, also known as the body or shaft, is the Tibia's middle section. The epiphysis is made up of two bone limbs, one closest to the thigh (also called superior or proximal) and the other closest to the foot (also called inferior or distal) (also known as distal or inferior). The Tibia is narrowest at the bottom, with a distal end that is small in size than the Proximal. This bone is composed of a soft and firm, spongy substance called Cortical bone and a hard, spongy substance called Cancellous bone or trabecular bone. Cancellous bone is a form of human tissue that is found throughout the body. It can also be found at the ends of large bones and in the pelvic bone columns. The tibia is divided into three architectural layers: cortical, trabecular, and marrow. Bone is a composite material composed of natural materials. By weight, bone is made up of around 60% mineral, 10% water, and 30% collagenous matrix. The quality of all of these aspects, as well as their relationships, have a major impact on the mechanical behavior of bone from the perspective of composite materials. The longitudinal axis of the bone is normally aligned with collagen and mineral crystals. Hence, the long axis of bone strength and stiffness is always greater [2, 3]. The Finite Element Method (FEM) is frequently used in biomechanics to estimate strain, load transfer in prosthetics, and the effects of internal stresses. [4].

It is well known that the vehicle industry has conducted extensive research on human life safety. In most cases, the study has concentrated on the upper body, and damage has been greatly minimised, for example, by installing airbags and strengthening the vehicle construction. However, the lower body, which is also an important part of the body, has received little attention until recently. According to a new vehicle crash research study, the driver's natural proclivity is to use the brakes as soon as possible before a collision. The lower leg should be the most affected by this action. This prompted investigations into the formation of human bone, its capacity to sustain an injury, and a rethinking of automotive design to lessen the power of impact on the lower bone.

## 2. LITERATURE REVIEW

The construction of subject-specific FEM of human bones has been scrutinised by many researchers in recent years. These are used to understand the clinical difficulties involving the reaction of bones when subjected to mechanical stress. Toth et al. [5] used a physical bending test and quantitative simulation on the tibia bone in an experimental investigation to examine the mechanical properties of adult canine bones. A FEM approach was used to correlate the results. Computed tomography (CT) was used to establish the shape and size of the Tibia bone, and ANSYS was used to do the numerical analysis. According to the findings, a deficiency in the Tibia proximal area bone has no significant influence on Tibia bone mechanical behaviour in the bending test. Fracture lines incline toward the defect zone somewhat. Bao et al. [6] analysed Tibial stress during the leaping moment using a FEM technique. The shape of the bone was determined using a CT scan. The stress and deformation were modelled using FEM software. The findings provide a theoretical framework for sports training, injury treatment, and rehabilitation. The stress, according to the data, lies in the centre of the Tibia bone. The tension on Tibia's foreshore is larger than the stress on Tibia's backside. Mehta et al. [7] used MRI and solid modelling software to create a 3D model to investigate the development of stress on the Tibia bone with static loads and the impact of different material qualities on stress. According to the behaviour and stress pattern, cancellous bone serves as a damper, transmitting maximal stress to compact bone. The stress analysis of the tibia when it was subjected to body weight in a static scenario was examined by Ghosh et al. [8]. The cross-section structure of the tibia at various points was utilised to generate a 3-D solid model of the tibia in SolidWorks. With the intention of finding the important tibia parts, ANSYS was utilised to assess the stress, strain, and displacement in the 3-D model. The important zone in terms of displacement is revealed to be the mating area between the tibia-fibula and the patella. The fibula has a crucial zone for stress between 25% and 40% of the way up from the bottom union region of the tibia and fibula. Gonzalez et al. [9] utilised CT information to create a 3D model of the tibia, which was then used to calculate the force required to initiate tibial torsional correction. Jyoti et al. [10] used FEA to do a quantitative study on the tibia bone. They conducted the vibration analysis for different boundary conditions. The outcome of the research demonstrates that the natural frequency of a tibia bone produced from magnesium alloy is lower than that of titanium alloy-based one. But its natural frequency is higher than that of a natural tibia bone. Bhaskar et al. [11] used a free body diagram to perform static analysis on the tibia for three distinct human postures (standing, staircase climb, and descending). The values obtained while standing and ascending and descending the stairs are added to FEA. The deformation and stress distribution was studied. MicroCT FEA paired with strain gauge data was utilised by Haisheng et al. [12] to estimate tissue-level stresses throughout the tibia. Liselore et al. [13] wanted to get a better understanding of the tibia and tibia plateau's anatomical variability. A total of 79 tibia CT images were analysed using principal component analysis. On the 3D models, morphologically relevant characteristics were assessed. Both sides of the bones had identical shape patterns, according to Nazl et al. [14], and there was no directional asymmetry in any bone type. Renaud et al. [15] discovered a substantial difference in the cortical thickness, internal diameter, and exterior diameter of men's and women's tibia bones, indicating a discriminant influence of sex on the tibia's cortical thickness, internal diameter, and external diameter. Yogeshet al. [16] studied bone remodelling in response to electromechanical stimulation in order to develop therapeutic treatments. For the first time, the finite element approach was used to evaluate piezoelectric bone in an open-source environment.

The purpose of all of the above research studies is to explore the behaviour of the tibia bone under several stressful circumstances. However, based on the literature study, the authors discovered that no research was done on a single family's male, female, and child boy. As a result, the aim of this study is to examine the effects of impact and static stress on the tibia bone of a male, female, and child boy from the same family. After acquiring a CT image of a typical Tibia bone, a 3D model was created and Finite Element Analysis (FEA) was performed using Ansys software.

## 3. MATERIALS AND METHODS

Film photography was traditionally used to examine scanned images. Converting 2D DICOM (“Digital Imaging and Communications in Medicine”) image data into 3D image data from a CT scan requires the following procedure: (a) Create a Region of Interest (ROI) by segmenting the data; (b) Translate the segmented data into a three - dimensional model; (c) Transfer the model in multiple formats for further processing, such as Finite Element Analysis. The recommended technique for doing Finite Element Analysis on a 3D model tibia bone using MIMICS (“Materialize Interactive Medical Image Control System”) and Ansys software is shown in Figure 2.

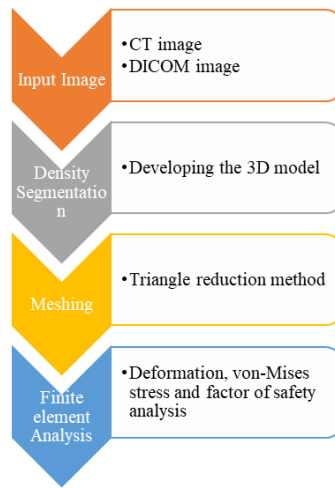


Figure 2. Block diagram depicting the creation of a 3D model from a DICOM picture.

MIMICS is a 3D medical image processing programme that may be used for 3D modelling and design. The version utilised in this study was MIMICS V14.12, and it was used to enhance and streamline the analytic process. A 2D DICOM CT scan with 48 cross-sectional slices and a thickness of 0.6 mm served as the starting point for the production of the 3D model. To begin, a ROI was created from the raw image using a segmentation algorithm that considered the distance between cavities, cavity size, and bone length. A segmented ROI from a 2D DICOM CT image is also imported, which imports and transforms all of the slices into a 3D data model. To reconstruct the bone separately, a manual editing technique is used based on the density mask.

The 3D modelling of the tibia bone is remeshed using the 3-matics technology. The gap ordinarily occupied by cartilages between the bones and the synovial fluid is not segregated in ROI. By separating the posterior section of the cartilages, the cartilages may be presented independently. In FEA, assigning different properties of materials depends on kinematic restrictions. The established core 3D models are subsequently transformed into 3-Matic system geometrical records, enabling 3D geometrical processes. In a three-dimensional object, little holes are considered undesirable triangles. Triangular reduction is a technique for improving triangle quality by lowering the number of defective triangles in the bone. Cavity filling techniques using a density mask have also been found to yield more independent and softer core 3D models. Polylines are used to allow the "Cavity Fill from Polylines" tool, which enables filling interior gaps simpler. The geometrical separation happens during the region-growing process by disconnecting the nearby mask, referred to as volume mesh, as shown in Figure 3.

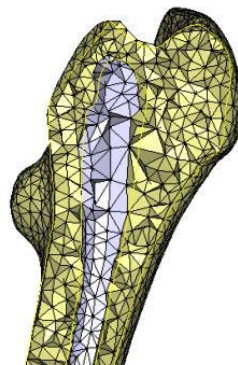


Figure 3. Volume mesh of Tibia bone.

Every slice of the CT scan image undergoes region-growing operations. Volume meshing has been employed in the 3-Matic system to increase and improve the quality of triangles. To achieve accurate results of the simulation, a volume mesh is created by adding material characteristics. If the three-dimensional structure is not sufficiently stated while applying load in ANSYS V14.5 software, an error will occur. During the region development period, the 3D structure of the tibia is fully defined. Surface mesh's sole aim is to improve the robustness of a 3D volume mesh design. The 3D data image is used to construct the segmented tibia bone, which is subsequently re-meshed in the 3-Matic platform.

To analyse the behaviour of the 3D model, it is loaded into ANSYS. To distinguish bone from bone structure, ANSYS recommends a minimum and maximum limit of 250 and 2000 Hounsfield units of volume soft tissues. By applying the load and material properties, as well as the boundary condition, FEA is utilised to determine the deformation and von Mises stress.

#### 4. RESULTS AND DISCUSSION

Lower extremity injuries are prevalent in traffic accidents, especially when an automobile and a pedestrian contact. Injuries to the bones, as well as the knees and ankles, are typical of this disease. A FEA report may be used to assess the outcomes of biomechanical testing and orthopaedic findings before conducting surgical procedures.

Generally, bones are two types of bone: anisotropic cortical bone on the surface and isotropic trabecular bone in the middle. The anisotropic material characteristics used in this study were taken from [17-19]. The material parameters of the tibia bone are listed in Table 1. Cortical bone is the thick surface layer of bone that forms a protective barrier around the internal cavity. The surface area of trabecular bone that is exposed to the bone marrow is bigger.

Table 1. Anisotropic material properties of tibia bones [17-19]

Material Properties	Cortical bone	Trabecular bone
Young's modulus (MPa)	$E_x = 18.400$ (longitudinal)	$E = 1.061$
Young's modulus (MPa)	$E_y = 7.000$ (transverse)	$E = 1.061$
Young's modulus (MPa)	$E_z = 8.500$ (radial)	$E = 1.061$
Poisson's ratio	$\nu_{xy} = 0.12$	$\nu = 0.225$
Poisson's ratio	$\nu_{yz} = 0.37$	$\nu = 0.225$
Poisson's ratio	$\nu_{xz} = 0.14$	$\nu = 0.225$

The finite element analysis was performed on a male, female, and child boy of a single household who is siblings and their ages are 23, 21, and 12 years, as stated in the conclusion paragraph of the literature review section. For the sake of finite element analysis, 15000 elements were constructed for each bone under consideration. To make the model more realistic, the thickness of the marrow, cortical and trabecular sections of the bone were included and their properties were collected from the literature [20-22]. Figure 4 depicts the entire tibia meshed model of a male, which is used in this investigation. The male tibia bone is 45 cm long and weighs 0.418 kg when the weight of this person is 78 kg. Solid 45 was given a tetrahedral shape with a 2mm element size. The bone was constructed and meshed using Solid 45 tetrahedral mesh components. The distal and proximal ends of the joint are also treated as one, and the tibia bone is treated as a single bone. In every degree of freedom, the distal end of the bone is fixed. At any point in time, the boundary conditions can be altered. The distal end of a male's tibia bone is entirely fixed in figure 5. Static analysis is used in this research. As indicated in Figure 6, the force is delivered to the proximal portion of the tibial plateau. Table 2 shows the loads considered on the proximal portion of the male tibia bone, which is obtained from the literature [8, 9, 23-25]. The deformation, von-Mises stress, and factor of safety of the tibia bone are calculated using simulation, and some screenshots are presented in Figures 7, 8, and 9. Table 2 summarises these figures. The male tibia bone was subjected to three sets of loads, with the associated deformation, von-Mises stress, and factor of safety listed in table 2. Finally, simulation results show that the male tibia bone failed at 5500 N.

Table 2. FEA simulation results of the male tibia bone.

S.No	Load (N)	Deformation (mm)	von-Mises Stress (MPa)	Factor of safety
1	735	0.33973	16.752	15
2	5000	6.2399	307.68	1.0335
3	5500	6.4711	319.08	0.99663

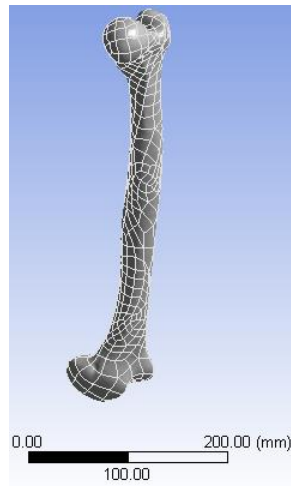


Figure 4. Tibia bone of a male with mesh.

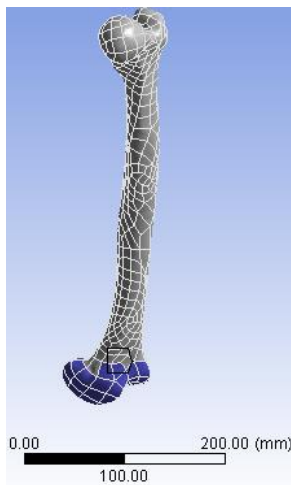


Figure 5. Completely fixed distal end of the tibia bone of male.

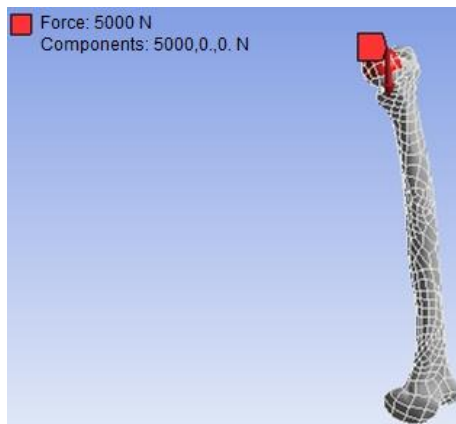


Figure 6. Load applied portion of the tibia bone of male.

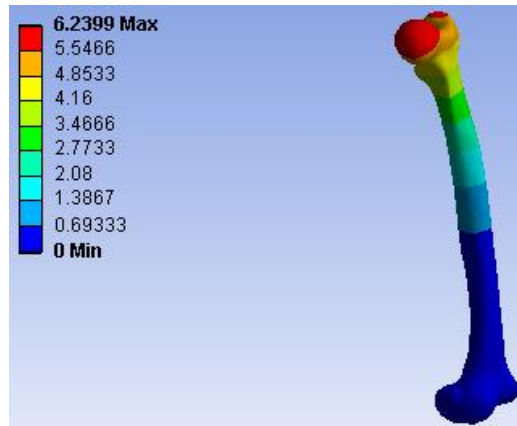


Figure 7. Deformation of the tibia bone of male.

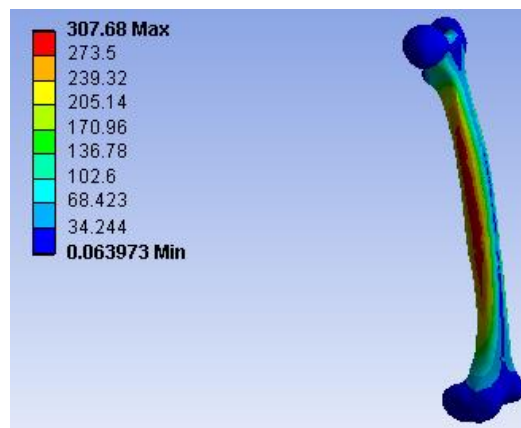


Figure 8. Von-Mises stress of the tibia bone of male.

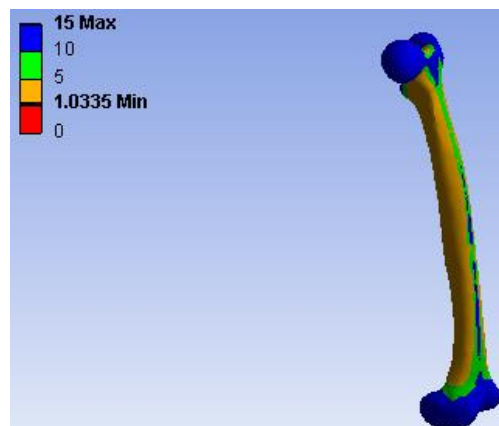


Figure 9. Factor of Safety of the tibia bone of male.

Similarly, FEA simulations on the female and child boy's tibia bones were performed using the loads indicated and retrieved from the literature [8, 9, 23, 24], and the corresponding deformation, von-Mises stress, and factor of safety are shown in table 3 and table 4, respectively. Figures 10, 11, 12, and 13 show representative screenshots of the female tibia bone loading, deformation, von-Mises stress, and factor of safety, respectively. Figures 14, 15, 16, and 17 show representative screenshots of the child boy's tibia bone loading, deformation, von-Mises stress, and factor of safety, respectively. The tibia bones of a female and a child boy are 42 cm and 32 cm long, respectively, while the weight of the matching human body is 53 kg and 32 kg. The tibia bone of the female and child boy both failed at 3500 N and 2000 N, respectively, in simulation.

Table 3. FEA simulation results of the female tibia bone.

S.No	Load (N)	Deformation (mm)	von-Mises Stress (MPa)	Factor of safety
1	637	0.35852	18.185	13.474
2	3150	4.784	242.66	1.0302
3	3500	5.0654	256.94	0.973

Table 4. FEA simulation results of child boy tibia bone.

S.No	Load (N)	Deformation (mm)	von-Mises Stress (MPa)	Factor of safety
1	245	0.17902	11.8	15
2	1850	3.6535	240.82	1.0381
3	2000	3.9857	256.94	0.94323

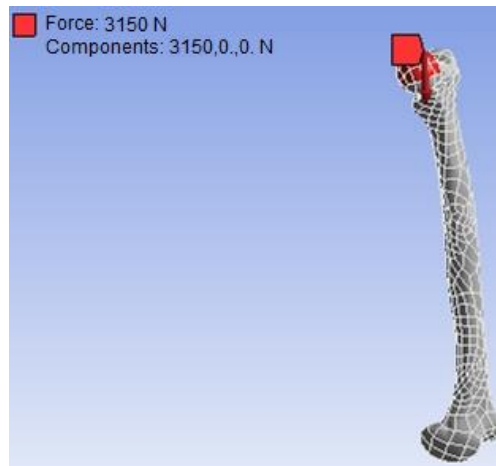


Figure 10. Load applied portion of the tibia bone of female.

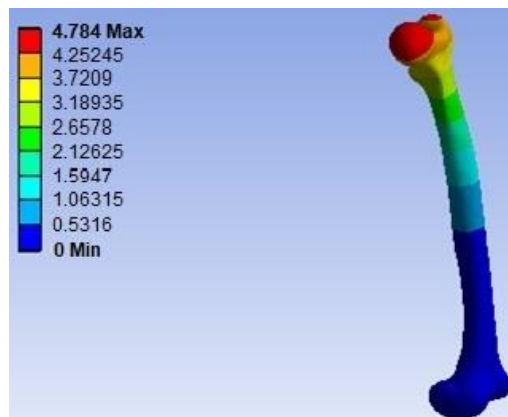


Figure 11. Deformation of the tibia bone of female.

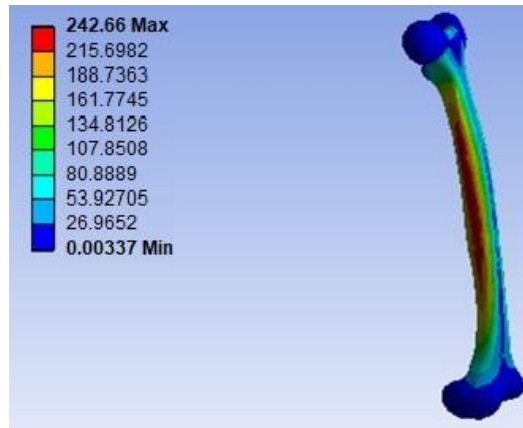


Figure 12. Von-Mises stress of the tibia bone of female.

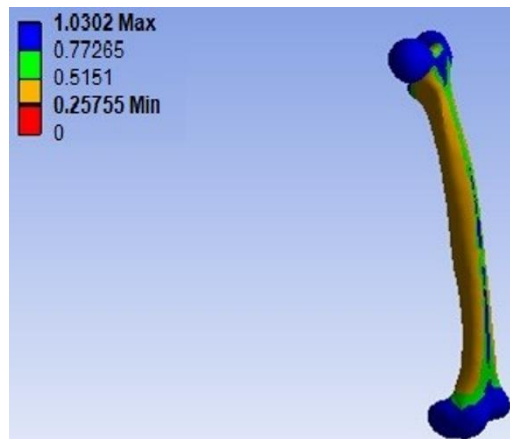


Figure 13. Factor of Safety of the tibia bone of female.

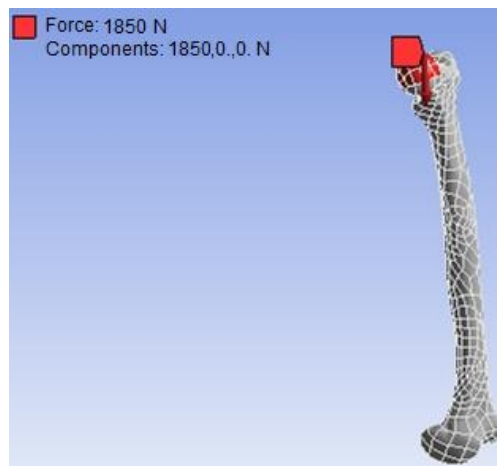


Figure 14. Load applied portion of the tibia bone of child boy.

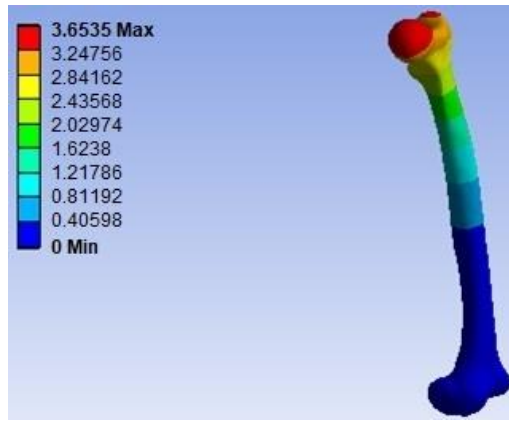


Figure 15. Deformation of the tibia bone of child boy.

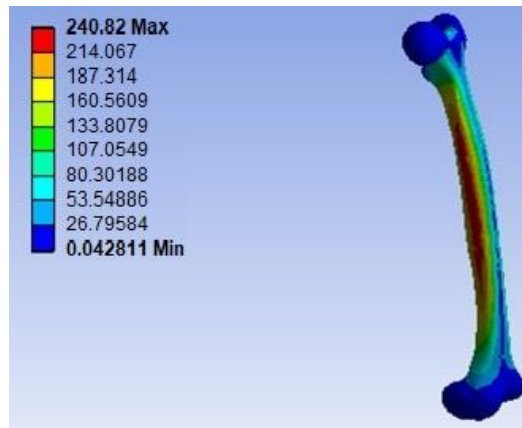


Figure 16. Von-Mises stress of the tibia bone of child boy.

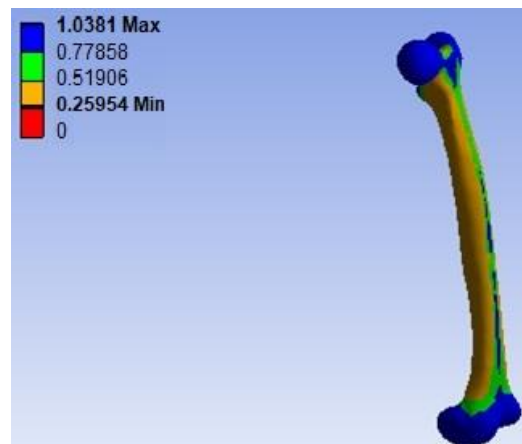


Figure 17. Factor of Safety of the tibia bone of child boy.

## 5. CONCLUSIONS

The 3D model was built from CT pictures of the tibia bone of a male, female, and child boy of a single-family aged 23, 21, and 12 years, respectively, using Mimics V14.12 software. Finite element analysis is performed on this 3D model. This model was then imported into the Ansys V14.5 programme for analysis and simulation. The static loading conditions were taken into account throughout the study. For various sets of loading situations, analytical simulation revealed the deformation, stress distribution, and factor of safety. The investigation was primarily conducted to determine the behavior of the Tibia bone under static loading circumstances and further to determine when the tibia bone breaks. The result of this study is that the 23-year-old male tibia bone will fail at almost 74 percent and 197 percent greater load than the sibling 21-year-old female and 12-year-old child boy tibia bone, respectively, based on the considered tibia bones of the male, female, and child boy. In addition, the 21-year-old female tibia bone is about 42% weaker than the sibling male tibia bone and 70% stronger than the sibling 12-year-old child boy tibia bone. Furthermore, the tibia bone of a 12-year-old child boy is about 66 percent and 42 percent weaker than that of a sibling, a 23

and 21 year old male and female, respectively. As a result of this research, it is known how much the sibling's tibia bone is weaker or stronger. Finally, this research may benefit orthopaedic surgeons in determining the load-bearing capability of the tibia bone in a single family's male, female, and child boy.

## REFERENCES

- [1]. <https://en.wikipedia.org/wiki/Tibia>. (accessed on 08 April 2022).
- [2]. Hasegawa K, Turner C.H, and Burr D.B., Contribution of collagen and mineral to the elastic anisotropy of bone, *Calcified Tissue International* 55 (1994) 381–386.
- [3]. Sasaki N, Matsushima N, Ikawa T, Yamamura H and Fukuda A., Orientation of bone mineral and its role in the anisotropic mechanical properties of bone-transverse anisotropy, *Journal of Biomechanics* 22 (1989) 157–164.
- [4]. S. Radzi, M. Uesugi, A. Baird, S. Mishra, M. Schuetz, and B. Schmutz, Assessing the bilateral geometrical differences of the tibia – Are they the same, *Medical Engineering & Physics* 36 (2014) 1618 – 1625.
- [5]. M. Toth Tascau, M. Drucean and L. Rusu, Biomechanical behavior of canine tibia based on bending tests and numerical analysis, 5th International Symposium on Applied Computational Intelligence and Informatics, University of Timisoara, mechatronics Department, Timisoara, Romania, (2009) 129-132.
- [6]. Chun-yu Bao and Qing-hua Meng, Three-Dimensional Finite Element Analysis of the Tibia Stresses during Jumping Momnet, 2010 International Conference on Computational and Information Sciences, Tianjin University of sport, China (2010) 756-759.
- [7]. B.V. Mehta and S. Rajani, Finite Element Analysis of The Human Tibia, *Transactions on Biomedicine and Health*, 2 (1995).
- [8]. M. Ghosh, B. U. Chowdhury, M S Parvej and A.M. Afsar, Modeling and Analysis of Elastic Fields in Tibia and Fibula. AIP Conference Proceedings. 1919 (2017) 020016-1 - 020016-7.
- [9]. R. A. Gonzalez-Carbonell, A. Ortiz-Prado, V. H. Jacobo-Armendariz, Y. A. Cisneros-Hidalgo and A. Alpi'zar-Aguirre, 3D patient-specific model of the tibia from CT for orthopedic use, *Journal of Orthopaedics*, 12 (2015) 11–16.
- [10]. Jyoti Joshi, Avi Raj Manral, Sudhanshu Maurya and Medhavi Vishnoi, Biomechanical analysis of human tibia bone based on FEA, *Materials Today: Proceesings*, 44 (2021) 1711-1717.
- [11]. Bhaskar Kumar Madeti, Chalamalasetti Srinivasa Rao and Bollapragada S.K. Sundara Siva Rao, Free body diagram and static finite element analysis of the human tibia, *International Journal of Biomedical Engineering and Technology*, 18(3) (2015) 290-299.
- [12]. Haisheng Yang, Kent D. Butz, Daniel Duffy, Glen L. Niebur, Eric A. Nauman and Russell P.Main, Characterization of cancellous and cortical bone strain in the in vivo mouse tibial loading model using microCT-based finite element analysis, *Bone*, 66 (2014) 131-139.
- [13]. Liselore Quintens, Michiel Herteleer, Sanne Vancleef, Yannick Carette, Joost Duflou, Stefaan Nijs, Jos Vander Sloten and Harm Hoekstra, Anatomical Variation of the Tibia – a Principal Component Analysis, *Scientific Reports*, 9 (2019) 7649.
- [14]. Nazlı Tümer, Vahid Arbabi, Willem Paul Gielis, Pim A. de Jong, Harrie Weinans, Gabrielle J. M. Tuijthof and Amir A. Zadpoor, Three-dimensional analysis of shape variations and symmetry of the fibula, tibia, calcaneus and talus, *Journal of Anatomy*, 234(1) (2019) 132-144.
- [15]. Renaud Breda, Yves Godio-Raboutet, Ertı Mavreri and Lionel Thollon, Structural Analysis of the Human Tibia by pQCT, *Journal of Orthopedic Research & Physiotherapy*, 2(21) (2016).
- [16]. Yogesh Deepak Bansod, Maeruan Kebbach, Daniel Kluess, Rainer Bader and Ursula van Rienen, Computational Analysis of Bone Remodeling in the Proximal Tibia Under Electrical Stimulation Considering the Piezoelectric Properties, *Frontiers in bioengineering and biotechnology*, 9 (2021) 705199.
- [17]. B. Sepehri, A. R. Ashofteh-Yazdi, G. A. Rouhi and M. Bahari-Kashani, Analysis of the effect of mechanical properties on stress induced in tibia, 5th Kuala Lumpur International Conference on Biomedical Engineering 2011, IFMBE Proceedings, 35 (2011) 130–133.
- [18]. E. Taheri, B. Sepehri, and R. Ganji, Mechanical validation of perfect tibia 3D model using computed tomography scan, *Scientific Research*, 4 (2012) 877–880.
- [19]. M. O. Kaman, N. Celik and S. Karakuzu, Numerical Stress Analysis of the Plates Used to Treat the Tibia Bone Fracture, *Journal of Applied Mathematics and Physics*, 2 (2014) 304-309.
- [20]. Dieter Christian Wirtz, Norbert Schiffers, Thomas Pandorf, Klaus Radermacher, Dieter Weichert, Raimund Forst, Critical evaluation of known bone material properties to realize anisotropic FE-simulation of the proximal femur, *Journal of Biomechanics*, 33 (2000) 1325-1330.
- [21]. Yinwang Zhang, Wuxue Zhong, Haibo Zhu, Yun Chen, Lingjun Xu and Jianmin Zhu, Establishing the 3-D finite element solid model of femurs in partial by volume rendering, *International Journal of Surgery*, 11 (2013) 930-934.

- [22]. G Narayanaswamy, Bindu A Thomas, Finite Element Analysis of Tibia Bone Model, International Journal of Engineering and Advanced Technology, 9 (2019) 4607-4610.
- [23]. Pratik S. Thakre, K.S. Zakiuddin, I.A. Khan and M.S. Faizan, Finite element analysis of tibia bone, International Journal of Biomedical Engineering and Technology, 35 (2021) 318–339.
- [24]. G. Ulrich Exner, Pascal A. Schai, Tobias C. Bühler and Theodore I. Malinin, Salvage of Failed Osteoarticular Tibia Allografts with Knee Arthroplasties, Open Journal of Orthopedics, 10 (2020) 67-76.
- [25]. Koji Totoribe, Etsuo Chosa, Go Yamako, Hiroaki Hamada, Koki Ouchi, Shutaro Yamashita and Gang Deng, Finite element analysis of the tibial bone graft in cementless total knee arthroplasty, Journal of Orthopaedic Surgery and Research, 13, 2018.